ACS Macro Letters

Letter

pubs.acs.org/macroletters

Polymer Looping Is Controlled by Macromolecular Crowding, Spatial Confinement, and Chain Stiffness

Jaeoh Shin,[†,‡] Andrey G. Cherstvy,[†] and Ralf Metzler*[,†,§]

[†]Institute for Physics and Astronomy, University of Potsdam, 14476 Potsdam-Golm, Germany

[‡]Max-Planck Institute for the Physics of Complex Systems, 01187 Dresden, Germany

[§]Department of Physics, Tampere University of Technology, 33101 Tampere, Finland

Supporting Information

ABSTRACT: We study by extensive computer simulations the looping characteristics of linear polymers with varying persistence length inside a spherical cavity in the presence of macromolecular crowding. For stiff chains, the looping probability and looping time reveal wildly oscillating patterns as functions of the chain length. The effects of crowding differ dramatically for flexible versus stiff polymers. While for flexible chains the looping kinetics is slowed down by the crowders, for stiffer chains the kinetics turns out to be either decreased or facilitated, depending on the polymer length. For severe confinement, the looping kinetics may become strongly facilitated by crowding. Our findings are of broad impact for DNA looping in the crowded and compartmentalized interior of living biological cells.

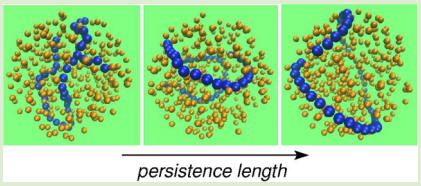

The cytoplasm of living biological cells is heavily crowded with various macromolecules[1−3] such as proteins, nucleic acids, cytoskeletal elements, cellular organelles, and internalized membrane structures. The volume fraction occupied by crowding agents can reach $\phi \sim 30-35\%$. Even in bacteria cells,[1] a polydisperse "zoo of proteins" at different abundances[4] nontrivially impact the kinetics of chemical reactions[5] and various other dynamic processes inside the cell[6] such as the aggregation of proteins and the folding of polypeptide chains into native protein structures.[7−9] Apart from this macromolecular crowding (MMC), living cells feature a highly compartmentalized interior, in which membrane-bound cellular organelles tune local concentrations of reactants and actively separate the reaction volume. Especially the DNA is often highly confined in biological systems, such as the spooled state of DNA inside capsid shells of bacteriophages[10] or the territorial reorganization of chromosomal DNA inside eukaryotic nuclei.[11]

DNA looping plays an important role in the compaction of the genome in prokaryotic nucleoids and the eukaryotic chromatin[12] as well as in gene regulation.[13] For protein-mediated DNA bending on the nanoscale, the persistence of DNA is often relevant, while in contact formation between distal chromosomal domains the effective polymer is very long and can be considered as flexible. In particular, the delicate way how MMC and confinement compete to tune DNA looping is vital for the speed and robustness of genetic networks.[14,15] MMC and confinement also concur in studies of protein folding[16,17] and DNA conformational dynamics, which can be probed inside nanocavities and nanochannels.[18] Apart from its fundamental importance in polymer physics and biochemistry, the looping of polymer chains in the presence of MMC and confinement is thus relevant for molecular biology and biotechnology. It is the main focus of this letter.

The static and dynamic properties of confined polymers[19,20] were recently studied intensely by experimental,[21,22] theoretical,[10,23−31] and simulation[7,17,32−36] approaches. Polymer looping itself was studied in the presence of MMC in refs 17 and 37−43. Typically, MMC slows down the effective diffusivity of the reactants and enhances the solution viscosity and thus impedes looping. This is particular true for small crowders. However, it was found that larger crowders effect internal "cages" and thereby facilitate the looping dynamics.[35]

Here we examine the concurrent effect of MMC and confinement in a spherical cavity on the looping dynamics of linear polymers of varying flexibility within a model of explicitly simulated crowders. Snapshots of the chain-crowder system are shown in Figures 1 and S.1 for different chain stiffnesses. As we show in the following, the interplay of crowding and confinement together with the chain stiffness gives rise to remarkable effects for the polymer looping that delicately depend on the system parameters. In particular, for stiff chains the looping probability and kinetics are wildly varying functions of the chain length.

We use Langevin dynamics simulations of coarse-grained bead−spring polymer chains[34] and our recently developed in-house package to explicitly model crowding molecules in the *NVT*-ensemble.[35,44] Chain beads of diameter σ are connected by a finitely extensible nonlinear elastic (FENE) potential, U_{FENE}. The self-avoidance of the polymer segments is modeled by the purely repulsive Lennard-Jones (LJ) potential U_{LJ} (Weeks−Chandler−Andersen potential). To model polymer semiflexibility, we include the bending potential U_{b} with stiffness κ connected to the chain persistence length as $l_{\mathrm{p}} = \sigma\kappa/$

Received: November 7, 2014
Accepted: January 13, 2015
Published: January 21, 2015

DOI: 10.1021/mz500709w
ACS Macro Lett. 2015, 4, 202−206

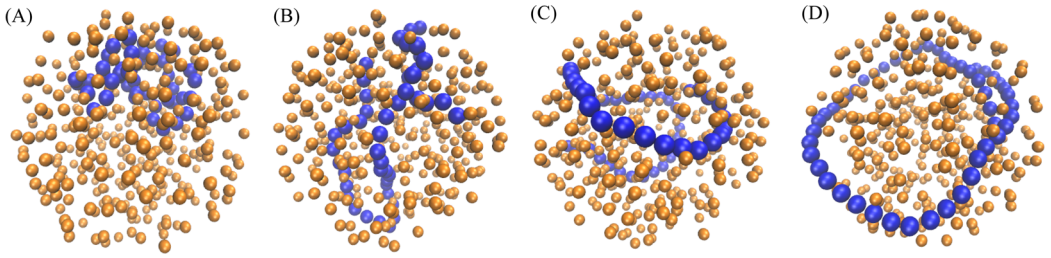

Figure 1. Snapshots of a polymer chain and crowders in a spherical cavity. The bending stiffness of the chain is (A) $\kappa/(k_BT) = 0$, (B) 4, (C) 16, and (D) 32. Parameters: chain length $n = 48$, crowder fraction $\phi = 0.1$, cavity radius $R = 7.5\sigma$, end-to-end cohesiveness $\epsilon_s = 5k_BT$, crowder diameter $d_{cr} = 1\sigma$. Video files illustrating the looping kinetics for these parameters are included in the SI. Crowder spheres are shown at 2/3 their actual radius for better visibility.

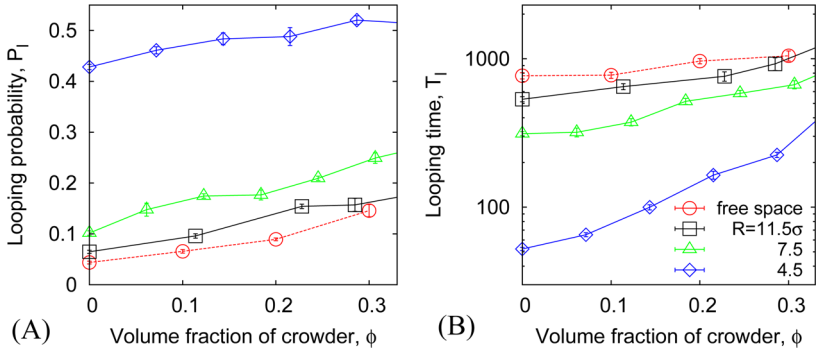

Figure 2. Looping probability P_l (A) and time T_l (B) as functions of MMC fraction ϕ for different confinement strengths computed for flexible chains with chain stiffness $\kappa = 0$. The error bars are as indicated; see SI for more details regarding their computation. Parameters: $n = 32$, $\epsilon_s = 5k_BT$.

(k_BT), where k_BT is the thermal energy. The bending stiffness is uniform along the polymer and no twist stiffness is considered. The reader is referred to the Supporting Information (SI) for details on the potentials, simulation procedure, and data analysis. We tested the simulations code for free-space semiflexible polymers and found good agreement (Figure S.2).

The two terminal monomers of the chain attract each other with an attractive LJ potential of energy ϵ_s (see SI) that mimics, for instance, the energetic gain for the formation of closed DNA hairpin structures via hydrogen-bond-interactions of complementary bases on ssDNA partners.[38] The energy gain counterbalances the loss of translational entropy upon loop formation by the end monomers. The effects of varying energy ϵ_s on the polymer looping kinetics in crowded unconfined solutions were recently studied.[35]

The crowders are modeled as purely repulsive LJ particles of diameter d_{cr}, set identical to the polymer bead diameter σ. The external spherical confinement acting on the polymer and crowders is implemented via a confining potential U_{conf} pointing inward from the sphere's boundary, see Figure S.3 for the crowder mean squared displacement inside the cavities. The volume fraction of crowders ϕ is computed with respect to the free space remaining after introducing the polymer into the cavity, $\phi = vN_{cr}/(4\pi R^3/3 - nv)$. Here N_{cr} is the number of crowding molecules in the system and $v = 4\pi(\sigma/2)^3/3$ is the monomer volume. We use the standard procedure from ref 35 to compute the looping probabilities and times of the terminal chain monomers, see also Figure S.4.

We first analyze the polymer distribution inside the confining cavity. As shown in Figure S.5, flexible chains without crowders ($\phi = 0$) explore the entire cavity, with a preference for the central part. In contrast, for stiff polymers the radial density distribution $\rho(r)$ shows a maximum close to the sphere surface, compare also ref 28. As crowders are added, flexible polymers become slightly depleted from the center of the cavity, while semiflexible chains with increasing ϕ acquire a pronounced peak close to $R - \sigma/2$: Semiflexible polymers are effectively pushed against the inner cavity surface by the depletion forces stemming from the crowders. MMC thus redistributes the polymer as if the cavity featured an attraction to the chain monomers, see also ref 45.

In contrast to the chain monomers, crowders are almost uniformly distributed in the cavity even at high concentrations ($\phi \sim 0.2$–0.3), Figure S.6A. For more severe confinement (small R), the distributions of both chain monomers and crowders feature clear oscillations due to progressive ordering; this effect is most pronounced in proximity of the cavity surface, Figure S.6B. Note that the polymer volume fraction is mostly chosen small compared to that of crowders, $\phi_p \ll \phi$.

The polymer end-to-end distribution $p(r)$ connected to the free energy as[35] $F(r) = -k_BT \log[p(r)]$ is shown in Figure S.7 for different radii R of the confining sphere in absence of crowders. The bimodal curves show a distribution of end-to-end distances, which consistently becomes narrower with decreasing R. Here, $r_c = 1.75\sigma$ is the cutoff distance, below which the chain is considered a closed loop, see SI and ref 35. The looping time T_l is defined as the time required for the chain ends to diffuse from the equilibrium extension $r = r_{eq}$ computed in the presence of confinement and MMC (from the free energy profiles of Figure S.7), to the final joint-ends extension with $r = r_f \sim r_c$. This makes the looping time definition strongly dependent on the extent of confinement, as expected on physical grounds. As the free energy profiles feature the same double-well shape also for semiflexible chains and for crowded solutions, see Figures S.8 and S.9, the current T_l definition is universal.

DOI: 10.1021/mz500709w
ACS Macro Lett. 2015, 4, 202−206

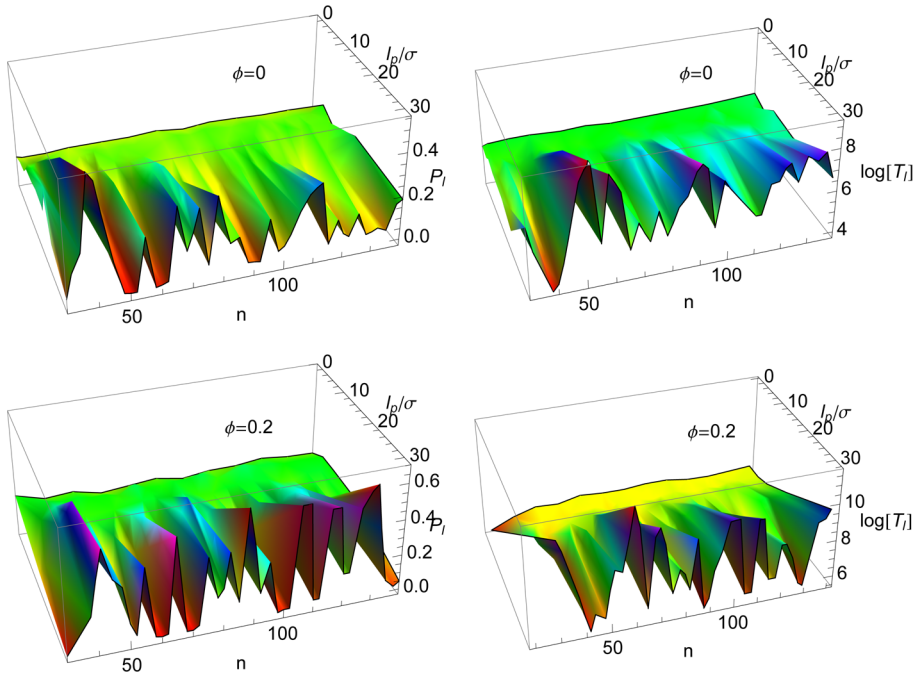

Figure 3. Variation of the looping probability $P_l(n, l_p)$ and looping time $T_l(n, l_p)$ as a function of the polymer length and the bending stiffness. Parameters: $R = 7.5\sigma$, $\epsilon_s = 5k_BT$, in absence of MMC (top panel) and at $\phi = 0.2$ (bottom panel). The looping time T_l is plotted in log scale. These three-dimensional plots include data points for $l_p/\sigma = 0$, 4, 8, 16, and 32 and the step size variation of the polymer length $\delta n = 2-5$. At $n \leq n^* = 30$, we observe almost no looping events within our simulation time, meaning that effectively $T_l(n) \to \infty$ and $P_l(n) \to 0$ (points not shown). The "hills" and "valleys" observed for the looping characteristics become more pronounced for stiffer chains. The total CPU time of a standard work-station to produce these graphs at a satisfactory resolution in the shown parameter space is about two months.

Figure S.10 shows results for the looping probability $P_l = \int_{\sigma}^{r_c} p(r')dr'$ and the looping time T_l. In free, uncrowded space, $T_l(n) \sim n^{2\nu+1}$,[46] where $\nu \approx 3/5$ is the Flory exponent for self-avoiding polymers. In ref 35 we confirmed this scaling for flexible polymers in crowded but unconfined conditions. Here, we focus on the effect of the compartment size R and the chain persistence length l_p. As demonstrated by Figure S.10, both in the absence and presence of crowders, the looping probability P_l approaches unity for small R and decreases with the cavity size roughly as $P_l(R) \sim R^{-3}$. $P_l(R)$ is thus inversely proportional to the available volume, reflecting the equilibrium character of $P_l(R)$. When the cavity is larger than the equilibrium end-to-end distance in free space, $R \gtrsim r_{eq}$, the looping probability saturates, the P_l of semiflexible chains being smaller than for flexible polymers due to the energetic penalty for chain bending. For $R \ll l_p$, the chain conformations are mainly determined by the external confinement and polymer flexibility effects become less important.

We find that the distribution of polymer looping times $p(T_l)$ in free and weakly confined crowded space is nearly exponential, see Figure S.11 and ref 35. Under severe confinement, $p(T_l)$ develops long tails, see Figure S.12. The average looping time $T_l(R)$ in absence of crowders increases as $T_l(R) \sim R^4$ and finally saturates for $R \gtrsim r_{eq}$ (Figure S.10B). In the presence of MMC the R-dependence of the looping time is roughly $T_l(R) \sim R^{2.5}$ (Figure S.10D) and thus significantly weaker than in its absence, consistent with the behavior shown in Figure 2B. The looping kinetics is thus facilitated under confinement. This is our first main conclusion of this study. Note that the scaling with R for P_l and T_l are in agreement with previous results for ideal and excluded-volume chains in spherical cavities without MMC.[26]

To unravel the interplay of confinement and MMC, we consider the looping probability and time versus ϕ at different R in Figure 2. We find i.a. that in strong confinement the effect of MMC onto the looping time is much stronger than onto the looping probability (shown in Figure 2A). For flexible chains, the MMC at $\phi = 0.2$ enhances the looping probability of $n = 32$ chains about 1.5 times, and the looping time grows about two times, almost independently of the chain length n, as detailed in Figure S.16A. The reader is referred to our recent study[35] for quantitative details on the viscosity of crowded solutions and looping of flexible chains: The looping kinetics is facilitated by external confinement, while antagonistically the crowding slows it down via enhancing the solution viscosity.

Our central result is presented in Figure 3, showing the looping probability P_l and time T_l as a function of the length n and the persistence length l_p of the polymer, without and with MMC. While for soft chains the n-dependence for both P_l and T_l appears fairly smooth, for growing chain stiffness wild variations become distinct. This is the second important conclusion of the current study. For larger l_p no looping occurs for chains shorter than some characteristic length, $n^* \approx 30$. This threshold naturally grows for stiffer chains, $n^*\sigma \sim l_p$, due to the growing bending energy for looping. Figure S.9 shows that the maxima of T_l in Figure 3 correspond to higher free energy barriers to accomplish the looping process, whereas fast looping events take place for smaller barriers, see Figure S.9.

How can this puzzling, wild behavior of the looping characteristics come about? To answer this question, we recall the steady-state results for the conformational statistics of semiflexible worm-like chains confined onto the surface of a sphere of radius R.[47] As a function of R, the mean end-to-end chain distance exhibits exponentially damped oscillations around the value $\langle r_0^2(R)\rangle = 2R^2$ with period $d_{WLC}(l_p, R) =$

DOI: 10.1021/mz500709w
ACS Macro Lett. 2015, 4, 202−206

$8\pi l_p R/(16l_p^2 - R^2)^{1/2}$.[47] For very stiff polymers, this period approaches $2\pi R$, corresponding to the lowest-energy chain ordering effected by wrapping in the equatorial plane of the sphere. For less stiff polymers, the correlations in the tangential orientations of the confined chain are progressively reduced and thus the period of the end-to-end oscillations d_{WLC} grows due to enhanced chain fluctuations. In large cavities and for relatively flexible chains satisfying the condition $R > 4l_p$ the correlations in the chain orientations disappear and the end-to-end distance monotonically increases to the saturation value $\langle r_0^2(R)\rangle$ as a function of the chain length.[47] We stress that these oscillations of the end-to-end distance of a confined semiflexible chain d_{WLC} effect regular variations in the looping characteristics.

Deviations of equilibrium chain conformations from the geodesic wrapping were rationalized with the Euler−Lagrange formalism in terms of the surface curvature of a closed semiflexible loop inside a sphere.[48] It was found that that for a chain completely attached to the sphere's surface, there exists an infinite number of distinct periodic states of the polymer that minimize the elastic energy. The incommensurability of the closed-chain length with the optimal wrapping strategy along the geodesic circle gives rise to the formation of various shapes, for example, tennis-ball-groove or rosette shapes, optimizing the energy,[49] see Figure S.13 and our results in Figure S.1, as well as the video files for stiffer chains, in the SI.

In the absence of MMC, Figure S.14 shows the average curvature $\bar{\kappa}$ along the compacted unlooped chain studied in our simulations as a function of polymer stiffness κ for the cavity radius $R = 7.5\sigma$. Up to the minimal possible curvature $1/R$ shown in the plot, the simulated data agree quite well with the scaling $\bar{\kappa}(\kappa) \sim \kappa^{-0.4}$ for two different chain lengths. Given this result, for very stiff polymers, whose length is a multiple of the equator length ($n\sigma \approx 2\pi RN$), the looping probability is thus expected to have local maxima, see also Figure S.1.[47] The structure of confined semiflexible chains will however deviate from the perfect spool-like arrangement. We thus observe from our simulations that both in uncrowded and crowded cavities the values of P_l and T_l are indeed strongly varying functions of the chain length, as seen in Figure 3. The effect is more pronounced for stiffer polymers.

More specifically, in absence of crowding the height of the wild variations of P_l and T_l in Figure 3 exceeds the mean value of these quantities for stiff chains. For more flexible chains the polymer ordering inside the cavity becomes less defined in the sense that these variations with the chain length become smaller and several chain conformations exist that optimize the free energy. This gives rise to the nonperiodic oscillations in the top panel of Figure 3. We point out that substantial variations of the looping properties with the chain length occur on length scales, which are significantly smaller than the period from the above ideal chain arguments, $d \ll d_{WLC}$. The extrema are due to the interplay of different optimal polymer conformations inside the cavity. As the chain persistence grows, the energy differences between these states become larger than the thermal energy and thus get reflected in variations of the looping characteristics with n, see Figure 3 and the video files in the SI. For very stiff chains some small polymer length variations δn make the polymers incommensurate to the geodesic circle and thus alter dramatically the looping properties, see Figure S.1. Figure S.15 shows additional detail for the dependence of P_l and T_l on the chain stiffness for different R. Note that the chain length of the extrema of P_l and T_l varies rather weakly with l_p, corresponding to different energy-optimizing configurations of the chain inside the cavity for varying κ.

The variations of P_l and T_l with the chain length are strongly anti-correlated for stiffer chains. This is particularly pronounced for short polymers, see Figure S.16 quantifying the looping characteristics along a cross-section of Figure 3 for soft and stiff polymers. This is the third conslusion of this letter. The effect is somewhat smeared out for longer chains, for which the height of the P_l and T_l variations decreases, see Figure S.16B. For a fixed cavity radius R, for even longer chains the looping rates get severely reduced. In this case, the motion of the chains is progressively restricted at higher polymer volume fractions ϕ_p. In Figure 3, however, $\phi_p < 3-5\%$, and these effects are not yet observable.

In the presence of MMC, we observe a similarly wild variation of the looping probability and time with the chain length (Figure 3). The positions of minima and maxima in P_l and T_l, however, are shifted as functions of the polymer length, compared to the results in absence of MMC. This is due to the tendency of crowding particles to push the polymer toward the cavity surface, effectively straightening out the fluctuations stored in the chain and effectively "rigidifying" the polymer and, thereby, shifting the position of the peaks in P_l and T_l. One can also think of this effect as of an effective increase of the cavity radius R. Figure 3 details the system behavior in a broad range of model parameters.

We presented Langevin dynamics simulations characterizing the looping behavior of semiflexible polymers inside a spherical cavity in the presence of MMC. Our first main result is that, as a function of the cavity size, the looping kinetics strongly depends on the presence of MMC, while equilibrium quantities such as the looping probability are only marginally affected (Figure 2A). Our second main result is the wild, anti-correlated variations of the looping probability and looping rates as a function of the chain length (Figures 3 and S.16): stiffer chains prefer to adopt different energy-optimized conformations inside the sphere and the transitions between them yield erratic looping characteristics as a function of the chain length. Under strong confinement the looping kinetics is dramatically facilitated by MMC, as compared to the free-space case (Figures 2B and S.15B). We expect that our results will impact the understanding of polymer looping, one of the most important molecular biochemical reactions, in the confined and crowded conditions typical for living biological cells.

■ ASSOCIATED CONTENT

Supporting Information

Details of the simulation procedure and additional figures and videos with description. This material is available free of charge via the Internet at http://pubs.acs.org.

■ AUTHOR INFORMATION

Corresponding Author

*E-mail: rmetzler@uni-potsdam.de.

Notes

The authors declare no competing financial interest.

■ ACKNOWLEDGMENTS

We thank J. Guven and P. Vazquez-Montejo for the files of Figure S.13 and E. Starostin for discussions on looping energetics. We acknowledge funding from the Academy of

DOI: 10.1021/mz500709w
ACS Macro Lett. 2015, 4, 202−206

Finland (FiDiPro scheme to R.M.), Deutsche Forschungsgemeinschaft (DFG Grant CH 707/5-1 to A.G.C.), and German Federal Ministry of Education and Research (BMBF Project to J.S.).

REFERENCES

(1) Zimmerman, S. B.; Minton, A. P. *Annu. Rev. Biophys. Biomol. Struct.* **1993**, *22*, 27.
(2) Weiss, M. *Int. Rev. Cell Mol. Biol.* **2014**, *307*, 383.
(3) Denton, A. R. *Int. Rev. Cell Mol. Biol.* **2014**, *307*, 27.
(4) McGuffee, A. R.; Elcock, A. H. *PLoS Comp. Biol.* **2010**, *6*, e1000694.
(5) Echeverria, C.; Kapral, R. *Phys. Chem. Chem. Phys.* **2012**, *14*, 6755.
(6) Schreiber, G.; Haran, G.; Zhou, H. X. *Chem. Rev.* **2009**, *109*, 839.
(7) Cheung, M. S.; Klimov, D.; Thirumalai, D. *Proc. Natl. Acad. Sci. U.S.A.* **2005**, *102*, 4753.
(8) Guo, M.; Xu, Y.; Gruebele, M. *Proc. Natl. Acad. Sci. U.S.A.* **2012**, *109*, 17863.
(9) Zhou, H. X.; Rivas, G.; Minton, A. P. *Annu. Rev. Biophys.* **2008**, *37*, 375.
(10) Marenduzzo, D.; et al. *Proc. Natl. Acad. Sci. U.S.A.* **2009**, *106*, 22269.
(11) Cremer, T.; Cremer, M. *Cold Spring Harbor Persp. Biol.* **2010**, *2*, a003889.
(12) Mirny, L. A. *Chromos. Res.* **2011**, *19*, 37.
(13) van den Broek, B.; et al. *Proc. Natl. Acad. Sci. U.S.A.* **2008**, *105*, 15738.
(14) Li, G. W.; Berg, O. G.; Elf, J. *Nat. Phys.* **2009**, *5*, 294.
(15) Tan, C.; et al. *Nat. Nanotechnol.* **2013**, *8*, 602.
(16) Mittal, J.; Best, R. B. *Proc. Natl. Acad. Sci. U.S.A.* **2008**, *105*, 20233.
(17) Denesyuk, N. A.; Thirumalai, D. *J. Am. Chem. Soc.* **2011**, *133*, 11858.
(18) Tree, D. R.; Wang, Y.; Dorfman, K. D. *Phys. Rev. Lett.* **2013**, *110*, 208103.
(19) Muthukumar, M. *Adv. Chem. Phys.* **2012**, *149*, 129.
(20) Micheletti, C.; Marenduzzo, D.; Orlandini, E. *Phys. Rep.* **2011**, *504*, 1.
(21) Leforestier, A.; et al. *Biophys. J.* **2011**, *100*, 2209.
(22) Reisner, W.; Pedersen, J. N.; Austin, R. H. *Rep. Prog. Phys.* **2012**, *75*, 106601.
(23) Marenduzzo, D.; et al. *Proc. Natl. Acad. Sci. U.S.A.* **2013**, *110*, 20081.
(24) Molineux, I. J.; Panja, D. *Nat. Rev. Microbiol.* **2013**, *11*, 194.
(25) Amitai, A.; Holcman, D. *Phys. Rev. Lett.* **2013**, *110*, 248105.
(26) Abrams, C. F.; Lee, N.-K.; Johner, A. *Macromolecules* **2006**, *39*, 3655.
(27) Lee, N. K.; Abrams, C. F.; Johner, A. *Europhys. Lett.* **2005**, *72*, 922.
(28) Gao, J.; Tang, P.; Yang, Y.; Chen, J. Z. Y. *Soft Matter* **2014**, *10*, 4674.
(29) Cherstvy, A. G. *Biopolymers* **2012**, *97*, 311.
(30) Sakaue, T. *Macromolecules* **2007**, *40*, 5206.
(31) Bhattacharyya, P.; Sharma, R.; Cherayil, B. J. *J. Chem. Phys.* **2012**, *136*, 234903.
(32) Kim, J.; Backman, V.; Szleifer, I. *Phys. Rev. Lett.* **2011**, *106*, 168102.
(33) Shin, J.; Sung, W. *J. Chem. Phys.* **2012**, *136*, 045101.
(34) Shin, J.; Cherstvy, A. G.; Metzler, R. *Phys. Rev. X* **2014**, *4*, 021002.
(35) Shin, J.; Cherstvy, A. G.; Metzler, R. *Soft Matter* **2015**, *11*, 472.
(36) Fošnarič, M.; et al. *Soft Matter* **2013**, *9*, 3976.
(37) Toan, N. M.; Marenduzzo, D.; Cook, P. R.; Micheletti, C. *Phys. Rev. Lett.* **2006**, *97*, 178302.
(38) Stiehl, O.; Weidner-Hertrampf, K.; Weiss, M. *New J. Phys.* **2013**, *15*, 113010.
(39) Marenduzzo, D.; Finan, K.; Cook, P. R. *J. Cell. Biol.* **2006**, *175*, 681.
(40) Watkins, H. M.; Simon, A. J.; Ricci, F.; Plaxco, K. W. *J. Am. Chem. Soc.* **2014**, *136*, 8923.
(41) Dupuis, N. F.; Holmstrom, E. D.; Nesbitt, D. J. *Proc. Natl. Acad. Sci. U.S.A.* **2014**, *111*, 8464.
(42) Nakano, S. I.; Miyoshi, D.; Sugimoto, N. *Chem. Rev.* **2013**, *114*, 2733.
(43) Ha, B.; Kim, J.; Jeong, H.; Jung, Y.; Jeong, C. *Soft Matter* **2015**, DOI: 10.1039/C4SM02198C.
(44) Shin, J.; Cherstvy, A. G.; Metzler, R. *New. J. Phys.* **2014**, *16*, 053047.
(45) Sirur, A.; Knott, M.; Best, R. B. *Phys. Chem. Chem. Phys.* **2014**, *16*, 6358.
(46) Toan, N. M.; Morrison, G.; Hyeon, C.; Thirumalai, D. *J. Phys. Chem. B* **2008**, *112*, 6094.
(47) Spakowitz, A. J.; Wang, Z.-G. *Phys. Rev. Lett.* **2003**, *91*, 166102.
(48) Guven, J.; Vazquez-Montejo, P. *Phys. Rev. E* **2012**, *85*, 026603.
(49) Winkler, R. G.; Cherstvy, A. G. *Adv. Polym. Sci.* **2014**, *255*, 1.

DOI: 10.1021/mz500709w
ACS Macro Lett. 2015, 4, 202−206